High Voltage Piezoelectric System for Generating Neutrons

Brady Gall, *Student Member, IEEE*, Scott D. Kovaleski, *Senior Member, IEEE*, James A. VanGordon, *Student Member, IEEE*, Peter Norgard, *Member, IEEE*, Baek Kim, *Member, IEEE*, Jae Wan Kwon, *Member, IEEE*, Gregory E. Dale, *Member, IEEE*

Abstract—Compact electrical neutron generators are a desirable alternative to radioisotope neutron sources. A piezoelectric transformer system is presented which has been used to achieve neutron production. The two primary components of the system include a piezoelectric transformer plasma source (PTPS), which produced a deuterium plasma for ion extraction, and a high voltage piezoelectric transformer (HVPT), which generated an accelerating potential in excess of 100 kV. The system was operated at a pressure of 700 μTorr with an external gas supply providing controlled deuterium flow to the differentially pumped PTPS. Synchronized AC signals were used to independently drive each of the piezoelectric devices in burst mode with a 1 Hz rep-rate and 1.3% duty factor. A timing offset between the two signals was used to decrease electrical loading effects and increase neutron flux. The mechanism for neutron production was the D(d,n)^{3}He nuclear reaction, occurring when deuterium ions from the PTPS accelerated toward and impacted a deuterium-impregnated Pd or Ti target adhered to the output terminal of the HVPT.

Index Terms—Piezoelectric Effect, Ion Sources, Neutron Production

I. INTRODUCTION

SINCE the introduction of the electronic neutron radiation source about 60 years ago, smaller, more efficient, more convenient sources of neutron radiation have been desired [**?**]. Electronic sources have many advantages over radioisotope sources, such as ^{252}Cf or AmBe, for a number of reasons, including narrow energy spectra, higher neutron flux, and the ability to be turned on and off. Sealed-tube neutron generators, for instance, can produce up to 10^8 n/sec for hundreds of hours. These neutron sources have led to advances in applications such as active interrogation and oil well logging.

The ideal neutron source for these applications is a lightweight, low power device that can be readily turned on and off. Devices using physical phenomena such as the pyroelectric effect have been demonstrated as methods for producing high voltage in compact form factors and others have even demonstrated neutron production [**?**], [**?**]. The piezoelectric effect is a related phenomenon which can be used to produce high voltage, with advantages including low weight, low power, and high efficiency [**?**]. Because of these characteristics, the piezoelectric effect is being investigated as a means to drive a compact, low power neutron source.

B. Gall, S. Kovaleski, J. VanGordon, P. Norgard, B. Kim, and J. Kwon are with the Department of Electrical and Computer Engineering, University of Missouri, Columbia, MO, 65211, USA e-mail: kovaleskis@missouri.edu

G. Dale is with the High Power Electrodynamics Group, Los Alamos National Laboratory, Los Alamos, NM 87541, USA e-mail: gedale@lanl.gov

This paper discusses a system for producing neutrons, which consists of a coupled configuration of two piezoelectric transformers. The first transformer is a radial piezoelectric disk, which is used to form a deuterium plasma in a small, differentially pumped chamber. The second is a high voltage bar-shaped Rosen-like transformer, which provides an accelerating potential. Deuterons are extracted from the plasma source and accelerated into a deuterium-impregnated target mounted on the high voltage terminal of the bar transformer. Neutrons are produced at the target via the D-D fusion reaction, and experiments have shown that at rates of 4680 $\pm$ 1320 min^{-1} have been achieved.

II. BACKGROUND

The piezoelectric neutron source presented in this document used the D(d,n)^{3}He nuclear reaction. In this reaction, an ionized deuteron, *d*, is accelerated into a static deuterium atom, *D*, to produce a 2.45 MeV neutron, *n*, and an 820 keV helium isotope byproduct, ^{3}He [**?**]. The cross-section for the D(d,n)^{3}He reaction is strongly dependent on the energy of the projectile deuteron, as shown in Fig. **??** [**?**], [**?**].

Figure **??** shows that the cross-section for the D(d,n)^{3}He reaction non-linearly increases with the energy of the deuteron. At 1 keV, the cross-section is 6.7$\times10^{-18}$ Barns, which increases to 8.9$\times10^{-6}$ Barns at 10 keV. At 100 keV, the cross-section reaches 17$\times10^{-3}$ Barns. As deuteron energy increases beyond 100 keV, a less substantial increase in cross-section occurs. This relationship between deuteron energy and cross-section indicates that an accelerator designed to cause the D(d,n)^{3}He reaction should be designed to reach at least 100 kV for a reasonable reaction cross-section.

The piezoelectric effect was used to facilitate a compact, high voltage neutron source design. The piezoelectric effect is the property of certain materials to respond to electrical and mechanical forces [**?**]. Piezoelectric transformers (PTs) are devices which use the piezoelectric effect to increase the voltage of an applied AC voltage. When operated in vacuum, piezoelectric transformers have been demonstrated to reach output voltages of greater than 120 kV, which is sufficient for neutron production using the D-D fusion reaction [**?**].

Report Documentation Page		*Form Approved* *OMB No. 0704-0188*

Public reporting burden for the collection of information is estimated to average 1 hour per response, including the time for reviewing instructions, searching existing data sources, gathering and maintaining the data needed, and completing and reviewing the collection of information. Send comments regarding this burden estimate or any other aspect of this collection of information, including suggestions for reducing this burden, to Washington Headquarters Services, Directorate for Information Operations and Reports, 1215 Jefferson Davis Highway, Suite 1204, Arlington VA 22202-4302. Respondents should be aware that notwithstanding any other provision of law, no person shall be subject to a penalty for failing to comply with a collection of information if it does not display a currently valid OMB control number.

1. REPORT DATE **JUN 2013**	2. REPORT TYPE **N/A**	3. DATES COVERED **-**

4. TITLE AND SUBTITLE **High Voltage Piezoelectric System for Generating Neutrons**	5a. CONTRACT NUMBER
	5b. GRANT NUMBER
	5c. PROGRAM ELEMENT NUMBER
6. AUTHOR(S)	5d. PROJECT NUMBER
	5e. TASK NUMBER
	5f. WORK UNIT NUMBER

7. PERFORMING ORGANIZATION NAME(S) AND ADDRESS(ES) **Department of Electrical and Computer Engineering, University of Missouri, Columbia, MO, 65211, USA**	8. PERFORMING ORGANIZATION REPORT NUMBER

9. SPONSORING/MONITORING AGENCY NAME(S) AND ADDRESS(ES)	10. SPONSOR/MONITOR'S ACRONYM(S)
	11. SPONSOR/MONITOR'S REPORT NUMBER(S)

12. DISTRIBUTION/AVAILABILITY STATEMENT
Approved for public release, distribution unlimited

13. SUPPLEMENTARY NOTES
See also ADM002371. 2013 IEEE Pulsed Power Conference, Digest of Technical Papers 1976-2013, and Abstracts of the 2013 IEEE International Conference on Plasma Science. IEEE International Pulsed Power Conference (19th). Held in San Francisco, CA on 16-21 June 2013., The original document contains color images.

14. ABSTRACT
Compact electrical neutron generators are a desirable alternative to radioisotope neutron sources. A piezoelectric transformer system is presented which has been used to achieve neutron production. The two primary components of the system include a piezoelectric transformer plasma source (PTPS), which produced a deuterium plasma for ion extraction, and a high voltage piezoelectric transformer (HVPT), which generated an accelerating potential in excess of 100 kV. The system was operated at a pressure of 700 Torr with an external gas supply providing controlled deuterium flow to the differentially pumped PTPS. Synchronized AC signals were used to independently drive each of the piezoelectric devices in burst mode with a 1 Hz rep-rate and 1.3% duty factor. A timing offset between the two signals was used to decrease electrical loading effects and increase neutron flux. The mechanism for neutron production was the D(d,n)3He nuclear reaction, occurring when deuterium ions from the PTPS accelerated toward and impacted a deuteriumimpregnated Pd or Ti target adhered to the output terminal of the HVPT.

15. SUBJECT TERMS

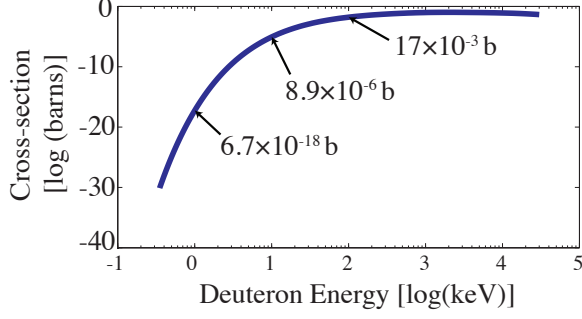| 16. SECURITY CLASSIFICATION OF:			17. LIMITATION OF ABSTRACT	18. NUMBER OF PAGES	19a. NAME OF RESPONSIBLE PERSON
a. REPORT **unclassified**	b. ABSTRACT **unclassified**	c. THIS PAGE **unclassified**	**SAR**	**5**	

Fig. 1: Cross-section for the D(d,n)3He nuclear reaction as a function of deuteron energy

III. EXPERIMENTAL SETUP

The crystals used to make the HVPT were $100\,\text{mm} \times 10\,\text{mm} \times 1.5\,\text{mm}$ -45-degree rotated y-cut lithium niobate slabs. Input electrodes, shown as gray regions on the top and bottom (not visible) surfaces on the left portion of the bar in Fig. **??**, were used to deliver electrical power to the crystal and applied using silver paint with a measured layer thickness of approximately $50\,\mu\text{m}$. A deuterated titanium foil measuring $10\,\text{mm} \times 2.5\,\text{mm}$ was adhered to the extremity of the output portion of the HVPT.
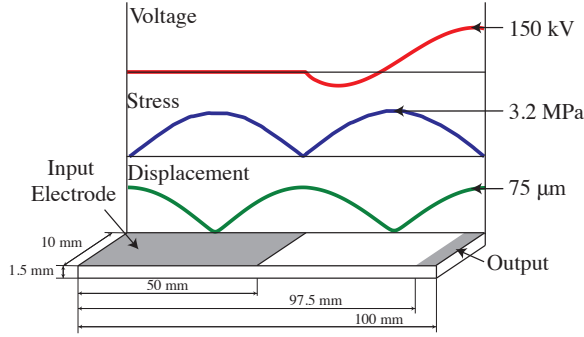
Fig. 2: Diagram of HVPT with linear profiles for voltage, stress, and displacement.

The crystals for the PTPS were disks of lithium niobate with 5 mm radius and 2 mm thickness, shown in Fig. **??**. Electrical energy was delivered through the thickness of the crystals via input electrodes on the top and bottom surfaces of the disk. The bottom electrode (not shown) spanned the entire area of the flat surface of the disk. The top electrode was annular and fixed at ground potential. The high voltage developed in the center portion of the top of the crystal. The disk was situated within a differentially pumped chamber, and plasma was formed at the high voltage surface. Deuterium was flowed into the PTPS between $5-10$ sccm and a $100\,\mu\text{m}$ aperture was used for ion extraction, shown in Fig.**??**.

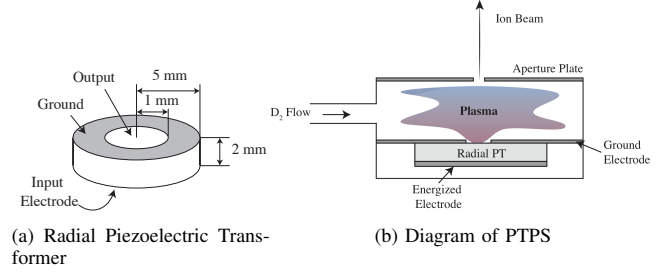(a) Radial Piezoelectric Trans-former

(b) Diagram of PTPS

Fig. 3: Diagram for radial PT and PTPS Chamber design

The system diagram to drive the coupled HVPT/PTPS neutron source is shown in Fig. **??**. Two individual drive circuits were required, with each transformer having its own circuit. The primary line was used to drive the HVPT and trigger the secondary line for the PTPS. A pair of Agilent 33210A function generators was used to produce the AC voltage to drive the piezoelectric crystals. A Stanford Research Systems DG535 digital delay pulse generator was used to offset the timing between the HVPT and the PTPS such that the ion beam current was produced at the end of the burst pulse for the HVPT. On the primary line, bursts of 6000 cycles at either 30.5 kHz or 60.7 kHz were generated and amplified by an Amplifier Research 25A250A 25 W, 43 dB rf power amplifier to drive the HVPT at $12\,\text{V}_{max}$. A Pearson 2877 current monitor with $1\,\text{V/A}$ output sensitivity measured the input current to the HVPT. On the secondary line, bursts of 7000 cycles at 385 kHz were generated by another AR 25A250A rf amplifier and fed into a $1-16$ step-up matching transformer to produce a drive voltage of $400\,\text{V}_{max}$. A Tektronix TDS 2024B oscilloscope was used to measure HVPT and PTPS input voltages and currents. The system diagram in Fig. **??** shows this setup.
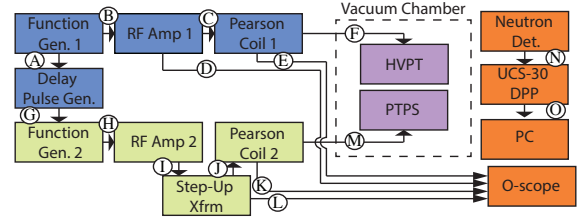

Fig. 4: System diagram for the coupled HVPT/PTPS neutron source. (A): 4 V TTL trigger; (B): $70\,\text{mV}_{max}$, 30 kHz or 60 kHz HVPT resonant frequency; (C, F): Input current to HVPT, $100-200\,\text{mA}_{max}$; (D): 1:10 measured HVPT Drive Voltage $10-20_{max}$; (E): Measured input current to HVPT; (G): Delay trigger for secondary line; (H): $400\,\text{mV}_{max}$ 385 kHz PTPS drive voltage; (I): $15\,\text{V}_{max}$ step-up transformer input voltage; (J,M): PTPS Driver current $100-200\,\text{mA}_{max}$; (K): Measured input current to PTPS; (L): 1:120 measured PTPS Drive Voltage; (N): Amplified neutron detector output; (O): Pulse-shaped digital output to PC.

An example of a typical pair of resonant burst pulses used to drive to the system is shown in Fig. **??**. The HVPT

burst pulse lasts 48 ms and is repeated at 1 Hz. During the HVPT pulse, the voltage decreases while the current increases, corresponding to a decrease in input impedance [**?**]. The PTPS burst pulse is delayed such that it occurs after the HVPT has reached steady-state. The PTPS burst pulse lasts only 13 ms because heating and excess stress can fracture the crystal for longer pulse lengths. Neutrons are only produced when both the HVPT and the PTPS are energized, resulting in an overall duty factor of 1.3 %.

A Pajarito Scientific He-3 neutron detector measuring 18.5×54.6 cm was used to capture neutron radiation. The detector has three 18-inch long, 1-inch diameter tubes pressurized to 4 atm. The gas mixture in the tubes is a 90 % He-3 and a 10 % proprietary mixture of methane and argon. An Ortek 659 5 kV bias supply provided 1.8 kV of drive voltage to the detector and a Canberra 2006 preamplifier was used as a preamplifier for the pulse detection. A USC-30 digital pulse processor was interfaced to a PC running USX x64 software to serve as an MCA for the neutron detector.
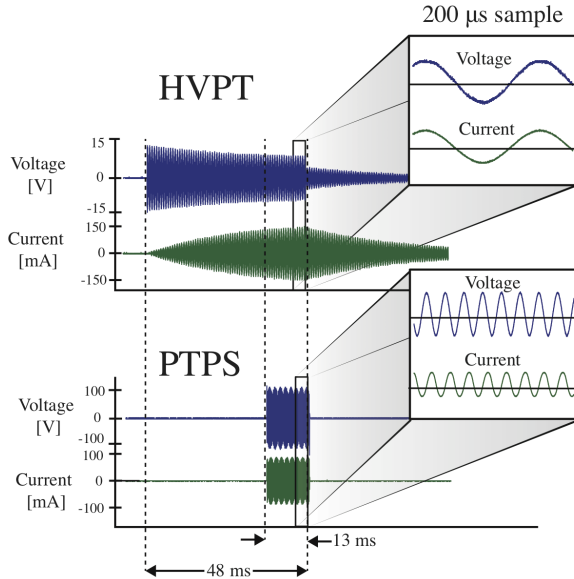

Fig. 5: Input voltage, and input current for a single synchronous burst of the HVPT and PTPS

Figure **??** shows the experimental setup for the piezoelectric neutron source. All experiments were conducted at base pressures between $3-7 \times 10^{-4}$ Torr. The HVPT was positioned such that its output terminal was aligned with the aperture of the PTPS and separated by a distance of 25 mm. The neutron detector was placed outside of the vacuum chamber at a distance of $10-20$ cm from the neutron source.
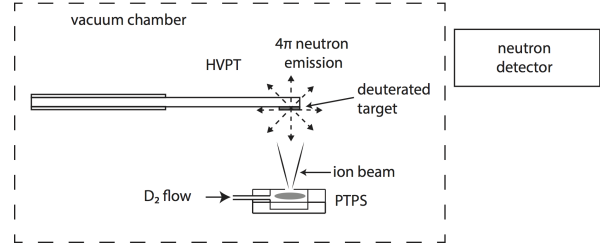

Fig. 6: Experimental setup for the piezoelectric neutron source

Two resonant modes were used to operate the HVPT, known as the fundamental mode and the second length-extensional mode or "mode 1" and "mode 2", respectively. Mode 1 is excited by a 30.5 kHz resonant frequency, with one displacement null occurring near the center of the bar. Mode 2 is excited by a 60.7 kHz drive, with two displacement nulls located at quarter-length positions. The mode 2 displacement profile is shown in Fig. **??** [**?**], [**?**]. In each case, the HVPT was clamped at the null points with acrylic mounting brackets to reduce mechanical damping. Figure **??** shows the mounting hardware used to clamp the HVPT for mode 2 operation. A photograph of the coupled HVPT/PTPS neutron system with mode 2 mounting hardware is shown in Fig. **??**.
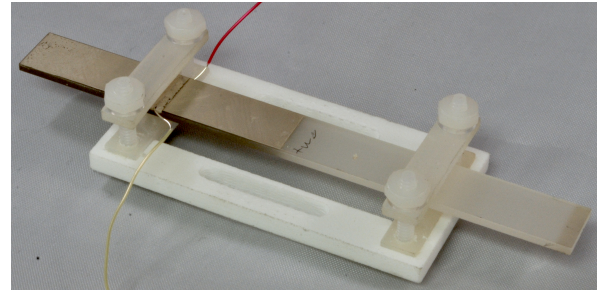
(a) Mode 2 HVPT mounting hardware
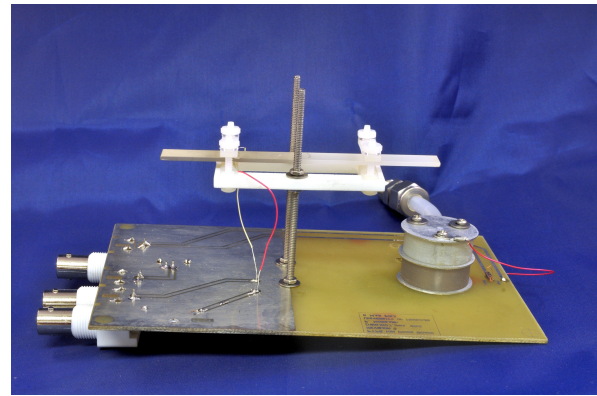
(b) Coupled HVPT/PTPS circuit board

Fig. 7: Photographs of hardware for HVPT mounting and circuit board

IV. RESULTS

The coupled HVPT/PTPS was tested as a neutron source with count rates significantly above measured background.

Neutrons were produced using the D(d,n)^{3}He nuclear reaction. Deuterium ions were extracted from the PTPS and accelerated to approximately 120 keV via the high voltage output of the HVPT.

Results with the HVPT-PTPS using mode 1 operation are tabulated and shown as tests 1 and 2 in table **??**. After these tests, the HVPT was removed from the vacuum chamber for examination. It was found that a small area of discoloration formed on the PTPS-facing surface of the HVPT. This was presumed to be caused by charged particle impingement on the surface of the HVPT. Figure **??** shows a photograph of this discoloration, measuring approximately 1 mm in diameter located 4.72 mm from the extremity of the bar and missing the deuterated target. This indicates that only a portion of the PTPS beam was incident on the target and that improved alignment between the PTPS and the HVPT target would further increase neutron yield.
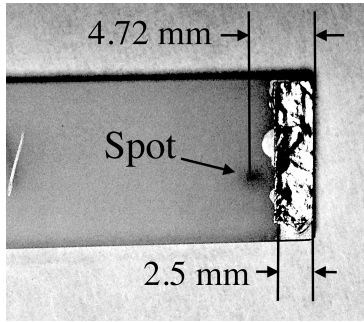

Fig. 8: Off-target beam spot

Electrostatic particle ray tracing analysis conducted in finite-element software was used to correct for misalignment between the PTPS ion source and the HVPT deuterated target. The vertical spacing between the PTPS and HVPT was fixed to 25 mm and the longitudinal positioning of the HVPT was swept over a range of distances to determine the optimal offset for beam placement on target. A diagram of the HVPT positioning offset is shown in Figure **??**.

Figure **??** shows the alignment configuration used in the tests 1 and 2, with no offset between the extremity of the HVPT and the PTPS aperture. In this case, the ion beam was deflected by 4.45 mm on the HVPT surface, which was consistent with the observed beam spot position shown in Figure **??**. Figure **??** shows the beam deflection with a 5 mm positioning offset. In this case, the beam spot was located 1.31 mm from the HVPT extremity which is within the region covered by the deuterated target. This analysis showed that precise HVPT positioning could increase ion beam intensity on target, increasing the probability of D-D fusion events and improving total neutron flux of the system.

The mode 2 mounting system was implemented to improve the positioning capabilities of the HVPT and target. By grasping the HVPT at two points along its length, the target was able to be more precisely and rigidly positioned as compared to the mode 1 mount, which only grasped the bar in the center and allowed for some freedom of motion at the extremity. The

experiment was repeated using the improved mounting system and with 5 mm target offset for beam alignment. The results from this experiment are shown in Fig.**??** and Table **??**.
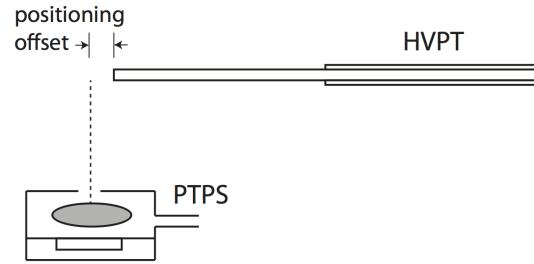
(a) Diagram of HVPT longitudinal positioning offset

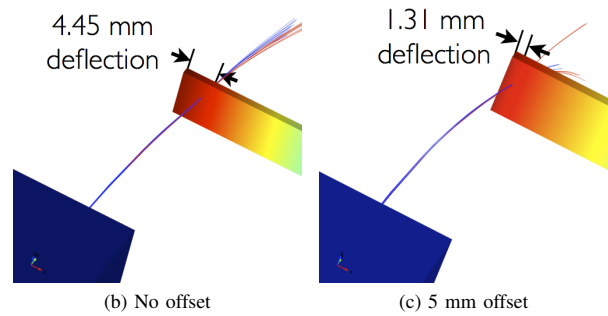(b) No offset   (c) 5 mm offset

Fig. 9: COMSOL model setup and results for improving ion beam intensity on target

Figure **??** shows a background-corrected time-resolved plot of neutron counts throughout the duration of a 2-hour long counting period. For approximately the first 30 minutes of operation, the count rate was low and indistinguishable from background. After 30 minutes, the neutron count rate increased above background and a steady increase in counts was measured. After 2 hours, the measured count rate was 4.22 standard deviations away from background, which corresponds to a confidence interval of greater than 99.9 %.
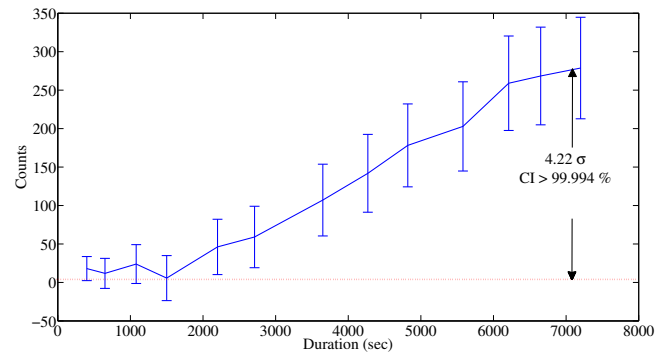

Fig. 10: Time-resolved neutron counts for Mode 2 HVPT-PTPS

Table **??** shows data collected for all three tests. Monte Carlo N-Particle (MCNP) code was used to model the overall

detection efficiency of the He-3 neutron detector used in this configuration [**?**]. Accounting for target/ion beam alignment showed to improve the count rate of the system. The count rates were 3200 ± 1100 min^{-1} for the non-aligned cases and 4680 ± 1320 min^{-1} for the aligned case.

TABLE I: Neutron count data collected during HVPT/PTPS operation corrected for detector and geometric efficiencies. Data collected over 2-hour long integrations and background is subtracted.

Test	HVPT Mode	Target aligned	Count Rate [cpm]	Source Rate [min^{-1}]
1	1	no	1.60 ± 0.55	3200 ± 1100
2	1	no	1.63 ± 0.55	3260 ± 1100
3	2	yes	2.34 ± 0.66	4680 ± 1320

V. CONCLUSION

A compact, low power piezoelectric system for producing neutrons was tested, showing that neutron count rates of over 4600 neutrons per minute were produced. The system used a coupled configuration of two piezoelectric transformers. The PTPS was a radial piezoelectric transformer situated in a differentially pumped chamber and produced a deuterium plasma for ion beam extraction. The HVPT was a bar-shaped PT, used for high voltage ion acceleration. A deuterated titanium film adhered to the output terminal of the HVPT provided a target for the $D(d,n)^3$He nuclear reaction. Electrostatic ray-tracing conducted using finite-element modeling showed that HVPT positioning is an important design consideration. Proper ion beam$-$target alignment required a 5 mm longitudinal offset to maximize beam intensity on target and improve neutron production rates. This was verified experimentally, showing increased neutron count rates for the aligned case over the non-aligned cases. [**?**]

ACKNOWLEDGEMENT

REFERENCES

[1] S. Nargolwalla and E. Przybylowicz, *Activation Analysis with Neutron Generators*. John Wiley Sons, 1973.
[2] J. A. Geuther and Y. Danon, "High-energy x-ray production with pyroelectric crystals," *Journal of Applied Physics*, vol. 97, May 2005.
[3] W. Tornow, S. Lynam, and S. Shafroth, "Substantial increase in acceleration potential of pyroelectric crystals," *Journal of Applied Physics*, vol. 107, no. 6, 2010.
[4] J. Yang, "Piezoelectric transformer structural modeling - a review," *Ultrasonics, Ferroelectrics and Frequency Control, IEEE Transactions on*, vol. 54, pp. 1154 –1170, june 2007.
[5] Atzeni, "Nuclear fusion reactions." Oxford University Press, April 2004.
[6] G. Miley, H. Towner, and N. Ivich, "Fusion cross section and reactivities," Tech. Rep. COO-2218-17, University of Illinois, Urbana, IL, 1974.
[7] B. Duane, *Fusion Cross Section Theory*. Brookhaven National Laboratory, 1972.
[8] T. I. of Electrical and I. Electronics Engineers, "Ieee standard on piezoelectricity." Standards Committee of the IEEE Ultrasonics, Ferroelectrics, and Frequency Control Society, March 1987.
[9] B. Gall, S. Kovaleski, J. VanGordon, and P. Norgard, "Investigation of the piezoelectric effect as a means to generate x-rays," *IEEE Transactions on Plasma Science*, January 2013.
[10] A. L. Benwell, *A high voltage piezoelectric transformer for active interrogation*. PhD thesis, Univeristy of Missouri, 2009.
[11] "Comsol multiphysics."
[12] K. Nakamura and Y. Adachi, "Piezoelectric transformers using linbo3 single crystals," *Electronics and Communications in Japan (Part III: Fundamental Electronic Science)*, vol. 81, no. 7, pp. 1–6, 1998.
[13] P. Norgard, B. Gall, and S. Kovaleski, "The efficiency of a helium-3 neutron detector evaluated using mcnpx," *Proceedings of the IEEE*, 2013.